Available online at www.sciencedirect.com
SCIENCE DIRECT®
Journal of Nuclear Materials 337–339 (2005) 1096–1100
journal of nuclear materials
www.elsevier.com/locate/jnucmat

A novel diagnostic for time-resolved spectroscopic argon and lithium density measurements

L. Schmitz *, P. Calderoni, A. Ying [1], M.A. Abdou

MAE Department, 43-133 Eng. IV, University of California, Los Angeles, CA 90095-1597, USA

Abstract

A new diagnostic technique for determining neutral gas and metal vapor densities over a wide pressure range with high time resolution is described. A compact, current-stabilized hollow cathode/anode discharge is use to ionize the gas and/or trace impurity to be analyzed. We report proof-of-principle operation of the diagnostic in a well characterized argon discharge in the pressure range 6.7–265 Pa. The intensity ratio of neutral and singly ionized argon lines ($I_{\mathrm{Ar\,I}}/I_{\mathrm{Ar\,II}}$) is shown to increase monotonically with the neutral argon density. In a second experiment, absolute neutral lithium vapor densities have been measured using this diagnostic.

PACS: 52.50.D; 07.60.R; 52.70; 52.25.Y
Keywords: Argon; First wall; Lithium; Neutrals; Spectroscopy

1. Introduction

The vacuum quality and neutral contaminants in fusion devices and inertial fusion energy (IFE) liquid chambers are usually determined by mass spectrometry. The required differential pumping limits the time resolution of quadrupole mass analyzers, and often absolute gas density measurements are difficult to obtain. In the framework of the IFE liquid chambers vapor clearing and condensation study at UCLA [1,2], partially ionized flibe (Li_2BeF_4) vapors are generated using a high-current electric discharge to simulate post-shot conditions. The condensation process is studied by measuring the total pressure of the condensing gases. To analyze the dynamics of recombination and composition of the gases and to investigate local gas thermodynamic properties such as vapor properties at the liquid/vapor interface, emission spectroscopy is used. Ionization of the gas in a hollow cathode/anode glow discharge permits absolutely calibrated lithium and beryllium density measurements. Hollow cathode discharges [3,4] have been extensively employed in light sources and as spectroscopic standards. They are relatively compact, robust, and easily assembled. Due to the high ionization efficiency of the hollow cathode/anode geometry, relatively high density, bright discharges are obtained, and the photon yield (and the achievable time resolution) for spectroscopic measurements is improved compared to a conventional glow discharge.

2. Experimental set-up

Fig. 1(a) shows a schematic of the experimental set-up for the proof-of-principle experiments. A modified

* Corresponding author.
E-mail addresses: lschmitz@ucla.edu (L. Schmitz), ying@fusion.ucla.edu (A. Ying).
[1] Tel.: +1 310 206 8815.

0022-3115/$ - see front matter © 2004 Elsevier B.V. All rights reserved.
doi:10.1016/j.jnucmat.2004.10.057

hollow cathode discharge (hollow cathode/anode discharge, HCA) is employed. The tungsten anode (0.63 cm in diameter) is arranged co-axially inside the hollow cathode, whereas in a conventional hollow cathode discharge (HCD) a ring anode is arranged outside the hollow cathode. The HCA is characterized by higher discharge voltage and offers enhanced ionization and excitation rates [5]. The HCA assembly is housed in a six-way port cross which can be baked at a temperature of up to 450 °C. A two-step pumping system is used for evacuation. For the work described in this paper a stainless steel cathode with a diameter $2a = 0.97$ cm was used. The length of the cathode tube is 2.6 cm. The discharge is powered by a 1 kV DC supply connected through a large resistor for current stabilization. Discharge currents of 2–20 mA are employed. The discharge breakdown voltage is determined by the Paschen law $V_{br} = f(pd)$, where p is the neutral gas pressure and d is the diameter of the (cylindrical) cathode [6]. From the Paschen curve, the minimum breakdown voltage in argon is obtained for $pd \sim 130$ Pa-cm. For $V < 600$ V, gas breakdown is possible in the pressure range $6\,\text{Pa} < p < 1300\,\text{Pa}$. With a larger diameter cathode, the accessible pressure range can be extended to below 0.13 Pa. Both cathode and anode are kept electrically isolated from the chamber ground in order to prevent gas ionization exterior to the discharge tube or at the vacuum high voltage feedthroughs. Sapphire/quartz windows allow end-on and side-on views of the plasma (the latter through a 2 mm opening in the cathode). A fiber–optic coupler and a compact spectrometer are used to record emissions in the visible and near-UV range (200–800 nm). The brightness of the discharge allows complete acquisition of this wavelength range in 5 ms. Typically we employ integration times of 20–100 ms to improve the signal to noise ratio. Much higher time resolution is possible if only one specific spectral line is monitored. A single, radially movable, swept Langmuir probe is used to record plasma density and electron temperature profiles. The probe current and voltage are recorded via fiber–optic links in order to provide electrical isolation from the digital oscilloscope used for recording the data.

3. Results and discussion

3.1. Discharge characterization in argon

Extensive Langmuir probe data were taken to characterize the plasma and to cross-reference the spectroscopic data. Fig. 1(b) shows a plot of the plasma density vs. argon neutral gas pressure for three radial positions. The bulk plasma density is found to increase initially with pressure (as the primary electrons traverse the cathode tube, the number of neutral atom ionization targets increases with pressure). As the pressure increases further the plasma density is found to decrease since the primary electron mean free path becomes smaller than the cathode diameter and gas ionization is less efficient and occurs closer to the cathode. As expected the electron temperature decreases slightly with increasing pressure as thermal energy transfer to the neutrals increases. The radial variation in bulk electron temperature is found to be weak.

3.2. Spectroscopic results

The emission spectrum from the HCA shows copious Ar II lines between 400 and 500 nm in addition to the expected presence of strong Ar I lines between 650 and 850 nm. In order to relate the emitted line intensities to the neutral and singly ionized argon populations, the excitation processes need to be investigated. The HCA is operated at low current (<20 mA) in order to limit

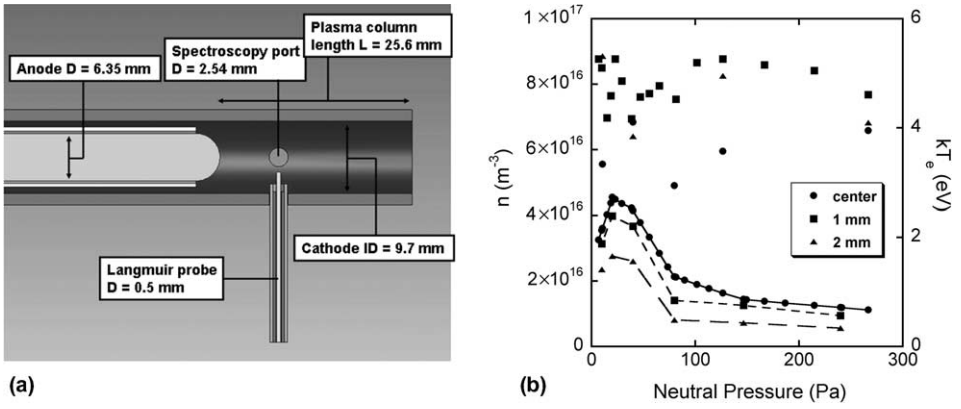

Fig. 1. (a) Cross-section of hollow cathode/anode geometry showing diagnostic access. (b) Plasma density evaluated from Langmuir probe ion saturation current, and bulk electron temperature from Langmuir probe characteristics vs. neutral argon pressure; data taken at three radial positions for a discharge current $I_D = 10$ mA.

the plasma density and avoid collisional-radiative effects and excitation of neutral argon from metastable levels. Ar I emissions at 811.5 nm ($3s^2 3p^5$ ($^2P^0_{3/2}$)4p–$3s^2 3p^5$ ($^2P^0_{3/2}$)4s, terms ^{2}[5/2]–^{2}[3/2]^0) and at 750.4 nm ($3s^2 3p^5$ ($^2P^0_{1/2}$)4p–$3s^2 3p^5$ ($^2P^0_{1/2}$)4s, terms ^{2}[1/2]–^{2}[1/2]^0) have been compared to evaluate the importance of metastable states [7]. The Ar I (750.4 nm) line originates from the $3s^2 3p^5$ ($^2P^0_{1/2}$)4p ^{2}[1/2] state which is primarily excited from the ground state, while the Ar I 811.5 nm line originates from the $3s^2 3p^5$ ($^2P^0_{3/2}$)4p ^{2}[5/2] level which is thought to be primarily populated from the $3p^5 4s$ $[3/2]^0_2$ metastable level at higher plasma density [8]. The intensity ratio of these two lines shows very little variation with plasma density (Fig. 2(a)), hence we can neglect excitation from metastable levels. Both bulk and primary electrons contribute to Ar I excitation (the integral is taken along the line of sight):

$$I_{\mathrm{Ar\,I}} \sim \left[\int_{-a}^{a} n n_0 \langle \sigma_{\mathrm{exe}} v_{\mathrm{th,e}} \rangle \, \mathrm{d}r + \int_{-r}^{r} n_{\mathrm{pr}} n_0 \langle \sigma_{\mathrm{exe}} v_{\mathrm{pr}} \rangle \, \mathrm{d}r \right]. \quad (1)$$

Here, n_{pr} and v_{pr} are the primary electron density and speed. If it is assumed that primary electrons are released by ions impacting the cathode, n_{pr} is roughly proportional to the plasma density $\langle n \rangle$. In addition, n_{pr} depends on the neutral argon density as shown previously [9,10]. Since primary electrons are born at the cathode and scattered by inelastic and elastic neutral collisions, the primary electron density profile becomes hollow with increasing neutral density. Calculating the line-integrated primary electron density as a function of neutral argon density from a 1-D fluid model, we conclude that for $\langle n \rangle$ = constant (fixed primary source rate) $\int n_{\mathrm{pr}} \, \mathrm{d}r / 2a \sim \langle n_{\mathrm{pr}} \rangle = n_0^{-1}$. Hence, if the plasma density is allowed to vary, $\langle n_{\mathrm{pr}} \rangle \sim \langle n \rangle / n_0$. Fig. 2(b) shows the Ar I (750.4 nm) line intensity, normalized by the plasma density, as a function of the neutral argon density. If only the first term in equation (1) would be important, then $I_{\mathrm{Ar\,I}} \sim n_0$. Primary electron excitation is not negligible at low neutral density, increasing emission. From the energy dependence of the excitation cross section for the Ar I (750.4 nm) line [11] the primary electron density is estimated as $n_{\mathrm{pr}} \sim 6.6 \times 10^{11} n / n_0$. This estimate is in agreement with previously published results [10].

Use of the HCA as a neutral density diagnostic requires a normalization to eliminate the plasma density dependence. It was found that the Ar II line intensities are proportional to the plasma density, as shown in Fig. 3(a) and (b) for the Ar II (488 nm) line ($3s^2$ $3p^4$ (^{3}P)4p^2 $D^0_{7/2}$–$3s^2$ $3p^4$ (^{3}P)4p $^2P_{3/2}$). Since the Ar II (488 nm) lower level is 17.14 eV above the Ar II ground state ($E_{\mathrm{exc}} \gg kT_e$) and the line intensity is proportional to the plasma density $\langle n \rangle$ rather than $\langle n \rangle^2$, we can conclude that emission is due to one-step excitation from neutral argon by primary electron impact [12]:

$$e_{\mathrm{pr}} + \mathrm{Ar}^0 \rightarrow \mathrm{Ar}^{+*} + 2e, \quad (2)$$

$$I_{\mathrm{Ar\,II}} \sim \int_{-a}^{a} n_{\mathrm{pr}} n_0 \langle \sigma_{\mathrm{exc}} v_{\mathrm{pr}} \rangle \, \mathrm{d}r. \quad (3)$$

The observed scaling $I_{\mathrm{Ar\,II}} \sim \langle n \rangle$ can be understood since $n_{\mathrm{pr}} n_0 \sim n$ as discussed above. Metastable Ar^{+*} states can be neglected, since only a small percentage of ions is produced in metastable states by the one-step process [13].

Fig. 4 shows the Ar I/Ar II line intensity ratio vs. the neutral argon density as measured by a calibrated baratron pressure gauge. This result demonstrates that the line intensity ratio increases monotonically with the neutral Ar density. With appropriate calibration absolute neutral density measurements can be obtained. As discussed above primary electrons contribute to Ar I excitation at low neutral pressure where the plasma density is higher ($n_{\mathrm{pr}} \sim n/n_0$).

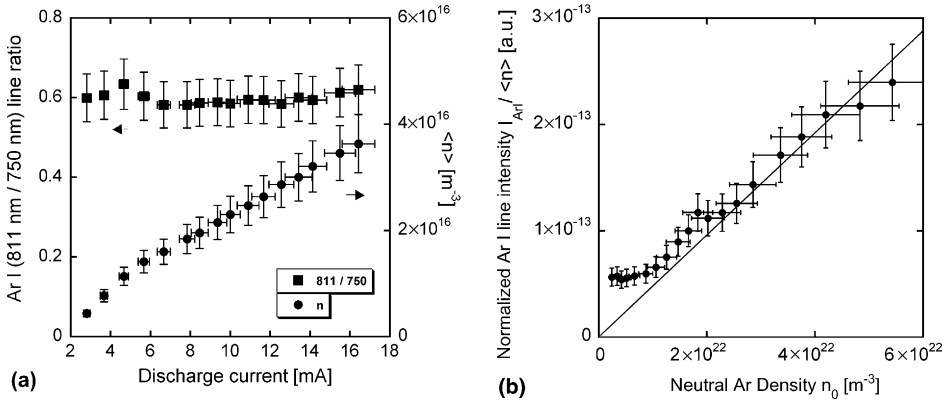

Fig. 2. (a) Ar I line intensity ratio 811.5 nm/750.4 nm and line-averaged plasma density $\langle n \rangle$ vs. discharge current; (b) normalized intensity $I_{\mathrm{Ar\,I}}/\langle n \rangle$ vs. neutral argon density n_0.

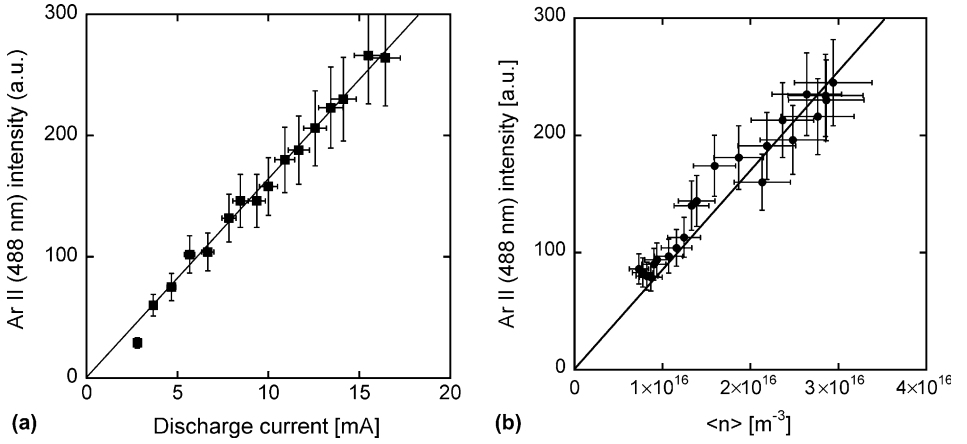

Fig. 3. (a) Ar II line intensity at 488 nm vs. discharge current; (b) Ar II line intensity (488 nm) vs. $\langle n \rangle$ for $I_D = 10$ mA (data for neutral pressures of 6.7–265 Pa are included).

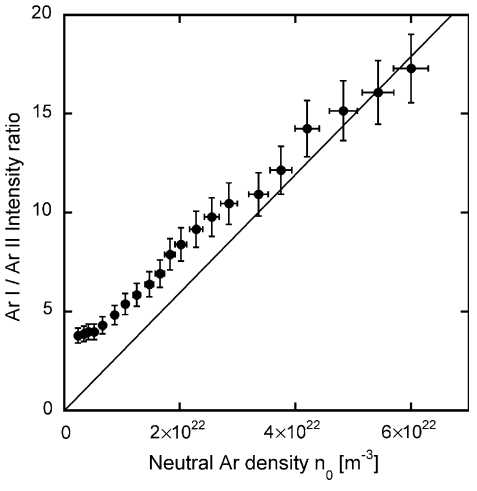

Fig. 4. Line intensity ratio Ar I (750.4 nm)/Ar II (488 nm) vs. neutral argon density ($I_D = 10$ mA).

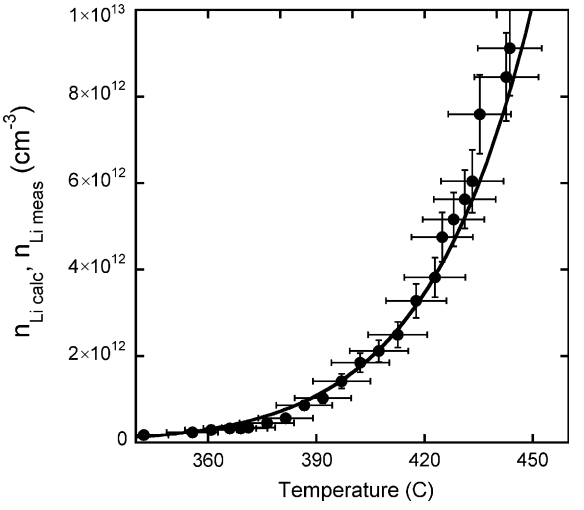

Fig. 5. Measured absolute Li density (circles) compared to the Li density (line) calculated from vapor pressure data as a function of Li temperature ($I_D = 10$ mA, neutral argon pressure 47 Pa).

3.3. Lithium vapor density measurements

In order to demonstrate the usefulness of the diagnostic method for the determination of metal vapor densities, a small block of lithium–aluminum alloy (with 3% lithium content) was installed in the experimental set-up at a distance of 10 cm in front of the hollow cathode assembly. An external heater was used to heat the Li–Al alloy to temperatures up to 450 °C (measured with a thermocouple). No aluminum contamination is present since the Al vapor pressure is several orders of magnitude below the Li vapor pressure. The chamber was kept at a temperature above 300 °C in order to avoid condensation of Li vapor. Argon gas (47 Pa) was used to initiate the plasma discharge. The Li I line intensity at 670.8 nm was recorded as a function of the Li temperature. The 670.8 nm emission results from ground-state electron impact excitation ($1s^2 2s \rightarrow 1s^2 2p$), and the lithium density can be directly determined from absolutely calibrated line intensity measurements, using the appropriate excitation cross-section [14] and the measured line-averaged plasma density:

$$n_{\mathrm{Li}} = \frac{P}{h\nu}\left[\frac{1}{2a}\int_{-a}^{a} n(r)\langle \sigma v_e \rangle \, \mathrm{d}r\right]^{-1}. \quad (4)$$

Here P is the emitted power per m^{-3}, h is Planck's constant and ν is the emitted frequency. Due to the low excitation energy of Li the bulk electrons dominate

excitation and primary electrons do not contribute significantly. Fig. 5 shows the measured line intensity as a function of the Al–Li temperature. The atomic Li density evaluated from the spectroscopic data closely matches the Li density obtained from vapor pressure data [15].

4. Conclusions

We have demonstrated the feasibility of absolute neutral density measurements in argon and lithium, using a compact modified hollow cathode discharge. This technique is useful for measuring the background gas density as well as trace impurities or metal vapor densities. Potential applications include the characterization of liquid first wall and divertor environments, condensation phenomena in ICF ion and laser beam lines, and radiative gas targets. Future work will concentrate on time-resolved measurements in a vapor condensation experiment [3], where lithium and beryllium partial pressures in the range of 1–100 Pa are expected. Other applications will be investigated, including operation of the device in a moderate magnetic field.

References

[1] P. Calderoni, A. Ying, T. Sketchley, M.A. Abdou, Fus. Technol. 39(N2) 711.
[2] P. Calderoni, UCLA PhD thesis, 2004.
[3] F. Paschen, Ann. Phys. 50 (1916) 901.
[4] G. Francis, The glow discharge at low pressure, in: S. Fluegge (Ed.), HdB Physik Bd XXII, Springer Verlag, Berlin.
[5] R.R. Arslanbekov, A.A. Kudryavtsev, R.C. Tobin, Plasma Sour. Sci. Technol. 7 (1998) 310.
[6] F. Paschen, PhD thesis, Strassburg, 1889.
[7] Moshkalyov, J.A. Dinitz, et al., J. Vac. Sci. Technol. B 15 (1997) 2682.
[8] J.-B. Boffard, G.A. Piech, M.F. Gehrke, et al., Phys. Rev. A 59-4 (1999) 2749.
[9] G. Helm, Z. Naturforschg. 27A (1972) 1812.
[10] F. Handle, W. Lindinger, F. Howorka, M. Pahl, Beitr. Plasmaphys. 24 (1984) 407.
[11] Z.M. Jelenak, Z.B. Velikic, J.V. Bozin, et al., Phys. Rev. E 47 (1991) 3566.
[12] M.J. Goeckner, J. Goree, T.E. Sheridan, Phys. Fluids B 3 (1991) 2913.
[13] P. Varga, W. Hofer, H. Winter, J. Phys. B 14 (1981) 1341.
[14] D.C. Griffin, D.M. Mitnik, Phys. Rev. A 64-8 (2001) 2947.
[15] An.A. Nesmeianov, in: J.I. Carasso (Ed.), Vapour pressure of the elements, Academic Press, NY.